TIFR/TH/03-10

Higgsino Dark Matter in a SUGRA Model with Nonuniversal Gaugino Masses

Utpal Chattopadhyay[(a)] and D.P. Roy [(b)]

[(a)] *Department of Theoretical Physics, Indian Association for the Cultivation of Science, Raja S.C. Mullick Road, Kolkata 700032, India*

[(b)] *Department of Theoretical Physics, Tata Institute of Fundamental Research, Homi Bhabha Road, Mumbai 400005, India*

Abstract

We study a specific SUGRA model with nonuniversal gaugino masses as an alternative to the minimal SUGRA model in the context of supersymmetric dark matter. The lightest supersymmetric particle in this model comes out to be a Higgsino dominated instead of a bino dominated lightest neutralino. The thermal relic density of this Higgsino dark matter is somewhat lower than the cosmologically favoured range, which means it may be only a subdominant component of the cold dark matter. Nonetheless, it predicts favourable rates of indirect detection, which can be seen in square-km size neutrino telescopes.

PACS: 13.40.Em, 04.65.+e, 14.60.Ef, 14.80.Ly

1 Introduction

The lightest supersymmetric particle (LSP) in the standard R-parity conserving supersymmetric model is the leading particle physics candidate for the dark matter (DM) of the universe [1]. The most popular supersymmetry (SUSY) breaking model is the minimal supergravity (SUGRA) model having universal scalar, gaugino masses and trilinear couplings at the GUT scale. Over most of the parameter space of this model the LSP is dominantly a bino ($\tilde{\chi}_1^0 \simeq \tilde{B}$) which does not couple to W or Z-boson. Hence they can only pair-annihilate via the exchange of superparticles like squarks or sleptons, $\tilde{B}\tilde{B} \xrightarrow{\tilde{q}(\tilde{l})} q\bar{q}(l^+l^-)$. The experimental limits on these particle masses, $m_{\tilde{q}} \gtrsim 200$ GeV and

$m_{\tilde{l}} \gtrsim 100$ GeV [2], imply a rather slow rate of pair annihilation. Consequently, the model predicts an over-abundance of the DM relic density over most of the parameter space [3]. This has led to several recent works, extending the SUSY DM investigations to nonminimal SUGRA models [4-7]. While many of them explore models with nonuniversal scalar masses, we shall concentrate here on nonuniversal gaugino mass models. In particular, we shall focus on a model leading generically to a Higgsino-like LSP. Because of its unsuppressed coupling to W and Z bosons the $\tilde{H}\tilde{H} \to W^+W^-, ZZ$ annihilation rates via s-channel Z-boson and t-channel Higgsino exchanges are large. Besides, there is a near degeneracy of the lighter neutralinos and lightest chargino masses in this case,

$$m_{\tilde{\chi}_1^0} \simeq m_{\tilde{\chi}_2^0} \simeq m_{\tilde{\chi}_1^\pm} \simeq |\mu|, \tag{1}$$

where μ is the supersymmetric Higgsino mass parameter. This leads to large coannihilation cross sections [8]. Consequently, the Higgsino DM density falls below the cosmologically favoured range [9],

$$0.05 < \Omega_m h^2 < 0.2, \tag{2}$$

where the lower limit corresponds to the galactic density of DM ($\Omega_m \simeq 0.1$) from rotation curves. Thus the Higgsino DM can only be a subdominant component of the galactic DM density. However, its large coupling to Z implies a large rate of capture inside the Sun. Hence, the model predicts a sizable indirect detection rate of Higgsino DM via high energy neutrinos coming from their pair annihilation in the solar core. This is much larger than the minimal SUGRA model prediction and should be detectable at the future neutrino telescopes, as shown below.

2 Non-Universal Gaugino Mass Model

SUGRA model with nonuniversal gaugino masses at the GUT scale have been discussed in many earlier works [10, 11, 12]. We shall only quote the main results here, focusing on the SU(5) GUT. In this model the gauge kinetic function depends on a nonsinglet chiral superfield Φ, whose auxiliary F-component acquires a large vacuum expectation value (vev). Then the gaugino masses come from the following dimension five term in the

Lagrangian:

$$L = \frac{< F_\Phi >_{ij}}{M_{Planck}} \lambda_i \lambda_j \tag{3}$$

where $\lambda_{1,2,3}$ are the $U(1)$, $SU(2)$ and $SU(3)$ gaugino fields i.e. the bino $\tilde{B}$, the wino $\tilde{W}$ and the gluino $\tilde{g}$ respectively. Since the gauginos belong to the adjoint representation of SU(5), Φ and F_Φ can belong to any of the irreducible representations appearing in their symmetric product, i.e.

$$(24 \times 24)_{symm} = 1 + 24 + 75 + 200 \tag{4}$$

The minimal SUGRA model assumes Φ to be a singlet, which implies equal gaugino masses at the GUT scale. On the other hand if Φ belongs to one of the nonsinglet representations of $SU(5)$, then these gaugino masses are unequal but related to one another via the representation invariants. Thus the three gaugino masses at the GUT scale in a given representation n are determined in terms of a single SUSY breaking mass parameter $M_{1/2}$ by

$$M^{G,n}_{1,2,3} = C^n_{1,2,3} M_{1/2} \tag{5}$$

where $C^1_{1,2,3} = (1,1,1)$, $C^{24}_{1,2,3} = (-1,-3,2)$, $C^{75}_{1,2,3} = (-5,3,1)$ and $C^{200}_{1,2,3} = (10,2,1)$. The resulting ratios of M_i^G's for each n are listed in Table 1.

n	M_3^G	M_2^G	M_1^G
1	1	1	1
24	1	$-3/2$	$-1/2$
75	1	3	-5
200	1	2	10

Table 1: Relative values of the SU(3), SU(2) and U(1) gaugino masses at GUT scale for different representations n of the chiral superfield Φ.

Of course in general the gauge kinetic function can involve several chiral superfields belonging to different representations of $SU(5)$ which gives us the freedom to vary mass ratios continuously. We shall explore such a possibility in a future work. But let us concentrate here on the representations 1, 24, 75 and 200 individually. While the singlet representation corresponds to universal gaugino masses, each of the nonsinglet representations corresponds to definite mass ratios and is therefore as predictive as the former.

These nonuniversal gaugino mass models are known to be consistent with the observed universality of the gauge couplings at the GUT scale [10–13]

$$\alpha_3^G = \alpha_2^G = \alpha_1^G = \alpha^G (\simeq 1/25) \tag{6}$$

Since the gaugino masses evolve like the gauge couplings at one loop level of the renormalisation group equations (RGE), the three gaugino masses at the electroweak (EW) scale are proportional to the corresponding gauge couplings, i.e.

$$\begin{aligned} M_1 &= (\alpha_1/\alpha_G) M_1^G \simeq (25/60) C_1^n M_{1/2} \\ M_2 &= (\alpha_2/\alpha_G) M_2^G \simeq (25/30) C_2^n M_{1/2} \\ M_3 &= (\alpha_3/\alpha_G) M_3^G \simeq (25/9) C_3^n M_{1/2} \end{aligned} \tag{7}$$

For simplicity we shall assume a universal SUSY breaking scalar mass m_0 at the GUT scale. Then the corresponding scalar masses at the EW scale are given by the renormalisation group evolution formulae [14]. A very important SUSY breaking mass parameter at this scale is m_{H_2} , as it appears in the EW symmetry breaking condition,

$$\mu^2 + M_Z^2/2 = \frac{m_{H_1}^2 - m_{H_2}^2 \tan^2\beta}{\tan^2\beta - 1} \simeq -m_{H_2}^2, \tag{8}$$

where the last equality holds for the $\tan\beta \gtrsim 5$ region, which is favoured by the Higgs mass limit from LEP [2]. Expressing $m_{H_2}^2$ at the right hand side in terms of the GUT scale mass parameters at a representative value of $\tan\beta = 10$ gives [14, 15]

$$\begin{aligned} \mu^2 + \frac{1}{2} M_Z^2 \simeq & -0.1 m_0^2 + 2.1 M_3^{G^2} - 0.22 M_2^{G^2} - 0.006 M_1^{G^2} + 0.006 M_1^G M_2^G + \\ & 0.19 M_2^G M_3^G + 0.03 M_1^G M_3^G, \end{aligned} \tag{9}$$

neglecting the contribution from the trilinear coupling term at the GUT scale. Moreover, the coefficients vary rather mildly over the moderate $\tan\beta$ region. Although we shall use exact numerical solutions to the two-loop RGE, two points are worth noting from this simple equation.

Firstly, eq.(9) gives a measure of fine-tuning from the required degree of cancellation between the dominant terms μ^2 and $M_3^{G^2}$ to give the right EW scale $M_Z^2/2$. The LEP limit on the lightest chargino mass, $m_{\tilde{\chi}_1^\pm} > 100$ GeV [2] implies

$$|\mu|, |M_2| > 100 \text{ GeV} \tag{10}$$

while eq.(9) implies

$$\begin{aligned} \mu^2 + M_Z^2/2 &\simeq 2.1 M_{1/2}^2 \text{ (for mSUGRA) and,} \\ \mu^2 + M_Z^2/2 &\simeq 1.4 M_{1/2}^2 \text{ (for n = 200 model)} \end{aligned} \tag{11}$$

Thus for the universal gaugino mass case of mSUGRA eqs.(7), (10) and (11) imply fine-tuning at least at the level of $\simeq 10$ [16]. On the other hand one sees from these equations that the fine-tuning problem is significantly alleviated in the nonuniversal models with $n = 75$ and 200, corresponding to $C_2^n = 3$ and 2 respectively [17].

Secondly, the universal gaugino mass model corresponds to $|\mu| > |M_2| > |M_1|$, which implies that the lighter chargino and neutralinos are dominantly gauginos with hierarchical masses -i.e. $m_{\chi_1^0} \simeq M_1$ and $m_{\chi_2^0, \chi_1^\pm} \simeq M_2 \simeq 2M_1$. There is however a narrow strip of very large m_0 region where the first term of eq.(9) pushes down $|\mu|$ towards the LEP limit as given in eq.(10). This is the so called focus point region [18], where the lighter chargino and neutralinos are mixed Higgsino-gaugino states. But, over the bulk of the parameter space the LSP is dominantly a $\tilde{B}$, which leads to an over-abundance of the DM relic density, as discussed earlier. One expects from Table 1 a similar result for the $n = 24$ model. In fact it predicts a larger hierarchy between the χ_1^0 and $\chi_2^0(\chi_1^\pm)$ masses, M_1 and M_2. Consequently the LSP is completely dominated by $\tilde{B}$ and can be relatively light. The SUSY DM phenomenology for this case has been discussed recently in Ref. [6, 7, 19]. In contrast we see from eqs.(7), (11) and Table 1 that the $n = 200$ model predict the opposite hierarchy $|\mu| < |M_2| < |M_1|$, while the $n = 75$ model has $|\mu| < |M_1| < |M_2|$. Thus the lighter chargino and neutralino states are Higgsino dominated and roughly degenerate (eq.(1)) over the bulk of the parameter space for both $n = 75$ and 200 models. This leads to a DM relic density somewhat below the cosmologically favoured range (eq.(2)). We should mention here that unlike the case of mSUGRA, there is no possibility of having stau coannihilations in the $n = 75$ and the $n = 200$ models. This is related to staus being significantly heavier than $m_{\tilde{\chi}_1^0}$ in these scenarios for all values of $\tan\beta$. This in fact originates from the gauge sector running of the slepton RGEs due to the specific gaugino mass nonuniversalities.

It is for the above reason that the Higgsino DM phenomenology of the nonuniversal SUGRA models, corresponding to $n = 75$ and 200 have not been explored in detail so far. We feel that this is important for two reasons: (i) Even though the Higgsino may be a subdominant component of the galactic DM density, its large coupling to Z-boson implies large rate of capture inside the Sun. Hence the model predicts a sizable indirect detection rate via high energy neutrinos coming from their pair annihilation inside the sun. Even after rescaling by the low DM density factor the indirect detection rate comes out to be larger than the minimal SUGRA predictions [20]. (ii) It is possible that the thermal relic density of the Higgsino DM is enhanced by either a modification of the freeze-out temperature of the standard cosmological model due to a quintessence field as suggested in Ref.[21] or by nonthermal production mechanisms of the type suggested in Ref.[22]. In that case it can be the dominant component of the galactic DM density. Therefore we have computed the indirect and direct detection rates both with and without rescaling.

3 Higgsino Dark Matter in the n=200 SUGRA Model

We shall concentrate on the nonuniversal SUGRA model corresponding to $n = 200$ because it can generate radiative electroweak symmetry breaking (EWSB) over a much wider range of parameters compared to the $n = 75$ case, the latter being restricted to have small $\tan\beta$ solutions only. Fig. 1 shows the allowed regions in the $m_0 - M_{1/2}(= M_3^G)$ plane for $\tan\beta$ =5, 10, 30 and 50. The area marked I at the top is disallowed because μ^2 falls below the LEP limit (eq.10) and then becomes negative, signalling the absence of EWSB. The area marked II at the bottom is disallowed because the Higgs potential becomes unstable at the GUT scale. We have chosen $\mu > 0$ since the $\mu < 0$ branch is strongly disfavoured by the $b \to s + \gamma$ branching ratio, along with the muon anomalous magnetic moment (a_μ) constraint. This figure shows that the $b \to s + \gamma$ constraint to be rather mild for $\mu > 0$. The lower limit from a_μ (not shown) is even milder.

We see from the contours of μ in Fig. 1 that one generally has $\mu < 500$ GeV in the model as anticipated. It also shows the gaugino component of the LSP,

$$Z_g = N_{11}^2 + N_{12}^2, \tag{12}$$

where

$$\tilde{\chi}_1^0 = N_{11}\tilde{B} + N_{12}\tilde{W} + N_{13}\tilde{H}_1 + N_{14}\tilde{H}_2. \tag{13}$$

We see that the bulk of the allowed parameter space corresponds to $Z_g < 10\%$, which means that the LSP is dominated by the Higgsino component to more that 90%. Finally Fig. 1 shows the contours of neutralino relic density $\Omega_\chi h^2$ which was computed using the micrOMEGAs of Ref. [23]. It is seen to generally lie below the lower limit of the cosmologically desirable range of eq.(2) by a factor of 2 to 4. This is due to the rapid pair annihilation processes $\tilde{H}\tilde{H} \to W^+W^-, ZZ$ via s-channel Z-boson and t-channel Higgsino exchanges, as mentioned earlier. Besides, the near degeneracy of the lighter chargino and neutralino masses (eq.1) leads to large coannihilations. In view of the mass degeneracy it is important to include radiative corrections to the $\tilde{\chi}_{1,2}^0$ and $\tilde{\chi}_1^\pm$ masses in the Higgsino LSP scenario [24]. We have included this using the code of Manuel Drees. But, it does not enhance the neutralino relic density significantly. It should be noted here that the dominant gaugino component of the LSP (eq.13) comes from $\tilde{W}$ instead of $\tilde{B}$, in view of the inverted mass hierarchy $\mu < M_2 < M_1$ in this model. Since, the winos have very similar annihilation mechanisms like the Higgsinos there is no increase in the relic density in the mixed Higgsino-gaugino region ($Z_g > 10\%$).

4 Indirect Detection Rates

Since the Z-boson couples only to the Higgsino component of neutralino, the $Z\tilde{\chi}_1^0\tilde{\chi}_1^0$ coupling is proportional to $N_{13,14}^2$ [25]. Moreover, the spin dependent force from Z-exchange is known to dominate the $\tilde{\chi}_1^0$ interaction rate with the solar matter, which is predominantly Hydrogen [1]. Hence the solar capture rate of the Higgsino DM is predicted to be enormously larger than the bino DM of the minimal SUGRA model. This implies in turn an enormously higher rate of pair annihilation, $\tilde{H}\tilde{H} \to W^+W^-(ZZ)$, since the capture and annihilation rates balance one another at equilibrium. The high energy neutrinos coming from W(Z) decay are expected to be detected at the large area neutrino telescopes like the

IceCubes [26] and the ANTARES [27] via their charged current interaction ($\nu \rightarrow \mu$). The resulting muons constitute the so called indirect DM detection signal. Fig. 2 shows the indirect signal rate contours over the full parameter space which was computed by using DARKSUSY of Ref. [28]. The signal contours are shown both with and without rescaling by a factor $\xi = \Omega_\chi h^2/0.05$ [29]. The denominator corresponds to $\Omega_m = 0.1$ which is the galactic DM relic density assumed in this computation. Even with rescaling one expects muon flux ϕ_μ of 5-100 events/km^2/year over practically the full parameter space of the model. In contrast the minimal SUGRA model predicts a $\phi_\mu < 1$ event/km^2/year over the entire parameter space, except for a very narrow strip at the $|\mu| = 100$ GeV boundary corresponding to a larger Higgsino content in the LSP [20]. The proposed large area neutrino telescopes like IceCube and ANTARES are expected to cover a detection area of 1 km^2. The irreducible background for these experiments, coming from the high energy neutrinos produced by the cosmic ray interaction with the solar corona is estimated to be $\phi_\mu \sim 5$ events/km^2/year [20]. Therefore these experiments can probe a signal of $\phi_\mu \gtrsim 5$ events/km^2/year, as expected over practically the full parameter space of this nonuniversal SUGRA model. It may be mentioned here that in the presence of some enhancement mechanism for the Higgsino DM relic density [21, 22], it can become the dominant component of the cold dark matter. This will enhance the indirect detection rate further, as indicated by the contours without rescaling.

5 Direct Detection Rates

For the sake of completeness we have computed the $\tilde{\chi}_1^0 p$ elastic scattering cross-sections in this model, which determine the signal rate in direct detection experiments. Both the spin-dependent and the spin-independent cross-sections have been computed using the DARKSUSY code [28].

The spin-dependent cross section is known to be dominated by Z-exchange. Therefore the spin-dependent cross-sections are much larger here compared to the minimal SUGRA model. Fig. 3 gives scatter plots of spin-dependent cross section against the LSP mass, both with and without rescaling for $\tan\beta$ =10 and 50. Even the rescaled cross-section is 1-2 orders of magnitude larger than the minimal SUGRA predictions [30]. Unfortunately, the direct detection experiments are not sensitive to the spin-dependent cross-section as they are based on heavy nuclei. For example the UKDMC detector is only sensitive to a spin-dependent cross section $\gtrsim 0.5$pb [30], which is much above any SUSY model prediction.

The spin -independent (scalar) cross-section is dominated by Higgs exchanges. Since the Higgs couplings to a $\tilde{\chi}^0\tilde{\chi}^0$ pair is proportional to the product of their Higgsino and gaugino components [25], they are suppressed for both Higgsino and gaugino dominated DM. Fig. 4 gives scatter plots of the scalar cross-section with and without rescaling for $\tan\beta$ =10 and 50. The upper range of the scatter-plots correspond to the mixed Higgsino-gaugino region ($Z_g > 10\%$) of Fig. 1, as expected. The cross sections without the rescaling factors are moderately larger than the minimal SUGRA prediction [30]. But the rescaled cross-sections are similar in size to the latter. Fig. 4 also shows that a significant part of the unrescaled cross-section lies above the discovery limits of the future CDMS [31] and GENIUS [32] experiments; but the rescaled cross-sections generally lie below these limits except for the mixed Higgsino-gaugino region. The DAMA [33] and present CDMS limits are also shown. In other words the upcoming experiments can detect the Higgsino DM if it is the dominant component of the galactic DM, but not if it is only a subdominant component of the latter.

6 Summary

We have investigated the dark matter phenomenology of a SUGRA model with nonuniversal gaugino masses. Its gauge kinetic function is a function of a nonsinglet chiral superfield, belonging to the 200-plet representation of SU(5). It is as predictive as the minimal SUGRA model and has less fine-tuning problem than the latter. It predicts a dominantly Higgsino LSP over the practically entire parameter space. The resulting thermal relic density of the Higgsino dark matter lies moderately below the cosmologically favoured range of eq.(2). Thus the Higgsino can only be a subleading component of the cold dark matter in the standard cosmological scenario. On the other hand its unsuppressed coupling to the Z-boson implies an enhanced rate of capture by the Sun. Consequently the predicted rate of indirect detection via high energy neutrinos coming from its pair-annihilation inside the Sun is much larger than the minimal SUGRA even after rescaling by the low density factor. This signal can be detected by the proposed km^2 neutrino telescopes like IceCube and ANTARES over practically the full parameter space of the model. For the direct detections the predicted rate after rescaling is rougly similar to the minimal SUGRA prediction.

We thank Manuel Drees for discussion and for the use of his radiative correction code for chargino and neutralinos.

References

[1] See e.g. G. Jungman, M. Kamionkowski and K. Griest, Phys. Rept. **267**, 195 (1996)

[2] K. Hagiwara *et al.* [Particle Data Group Collaboration], Phys. Rev. D **66**, 010001 (2002).

[3] See e.g. J. R. Ellis, A. Ferstl and K. A. Olive, Phys. Lett. B **532**, 318 (2002); U. Chattopadhyay and P. Nath, Phys. Rev. D **66**, 093001 (2002); H. Baer, C. Balazs, A. Belyaev, J. K. Mizukoshi, X. Tata and Y. Wang, arXiv:hep-ph/0210441; U. Chattopadhyay, A. Corsetti and P. Nath, arXiv:hep-ph/0303201.

[4] R. Arnowitt and B. Dutta, arXiv:hep-ph/0112157; R. Arnowitt and B. Dutta, arXiv:hep-ph/0210339.

[5] J. R. Ellis, T. Falk, K. A. Olive and Y. Santoso, Nucl. Phys. B **652**, 259 (2003).

[6] A. Corsetti and P. Nath, Phys. Rev. D **64**, 125010 (2001); U. Chattopadhyay, A. Corsetti and P. Nath, Phys. Rev. D **66**, 035003 (2002); A. Bottino, N. Fornengo and S. Scopel, Phys. Rev. D **67**, 063519 (2003); A. Birkedal-Hansen and B. D. Nelson, Phys. Rev. D **64**, 015008 (2001); A. Birkedal-Hansen and B. D. Nelson, arXiv:hep-ph/0211071; A. Bottino, F. Donato, N. Fornengo and S. Scopel, arXiv:hep-ph/0304080.

[7] V. Bertin, E. Nezri and J. Orloff, JHEP **0302**, 046 (2003).

[8] S. Mizuta and M. Yamaguchi, Phys. Lett. B **298**, 120 (1993).
Recent analyses with analytical results for coannihilations may be seen in: A. Birkedal-Hansen and E. Jeong, JHEP **0302**, 047 (2003); T. Nihei, L. Roszkowski and R. Ruiz de Austri, JHEP **0203**, 031 (2002).

[9] We considered a more conservative limit in our analyses than what has recently appeared in the following references: C. L. Bennett *et al.*, arXiv:astro-ph/0302207; D. N. Spergel *et al.*, arXiv:astro-ph/0302209.

[10] J. R. Ellis, K. Enqvist, D. V. Nanopoulos and K. Tamvakis, Phys. Lett. B **155**, 381 (1985); M. Drees, Phys. Lett. B **158**, 409 (1985).

[11] G. Anderson, C. H. Chen, J. F. Gunion, J. Lykken, T. Moroi and Y. Yamada, arXiv:hep-ph/9609457; G. Anderson, H. Baer, C. h. Chen and X. Tata, Phys. Rev. D **61**, 095005 (2000).

[12] K. Huitu, Y. Kawamura, T. Kobayashi and K. Puolamaki, Phys. Rev. D **61**, 035001 (2000).

[13] U. Chattopadhyay and P. Nath, Phys. Rev. D **65**, 075009 (2002).

[14] See e.g. M. Carena, M. Olechowski, S. Pokorski and C. E. Wagner, Nucl. Phys. B **426**, 269 (1994).

[15] S. Komine and M. Yamaguchi, Phys. Rev. D **63**, 035005 (2001).

[16] R. Barbieri and G. F. Giudice, Nucl. Phys. B **306**, 63 (1988). K. L. Chan, U. Chattopadhyay and P. Nath, Phys. Rev. D **58**, 096004 (1998).

[17] G. L. Kane and S. F. King, Phys. Lett. B **451**, 113 (1999).

[18] J. L. Feng, K. T. Matchev and T. Moroi, Phys. Rev. D **61**, 075005 (2000); J. L. Feng, K. T. Matchev and F. Wilczek, Phys. Rev. D **63**, 045024 (2001).

[19] G. Belanger, F. Boudjema, A. Cottrant, R. M. Godbole and A. Semenov, Phys. Lett. B **519**, 93 (2001).

[20] V. D. Barger, F. Halzen, D. Hooper and C. Kao, Phys. Rev. D **65**, 075022 (2002). See also J. L. Feng, K. T. Matchev and F. Wilczek, Phys. Rev. D **63**, 045024 (2001); A. Corsetti and P. Nath, Int. J. Mod. Phys. A **15**, 905 (2000).

[21] P. Salati, arXiv:astro-ph/0207396; F. Rosati, arXiv:hep-ph/0302159.

[22] B. Murakami and J. D. Wells, Phys. Rev. D **64**, 015001 (2001); T. Moroi and L. Randall, Nucl. Phys. B **570**, 455 (2000); M. Fujii and K. Hamaguchi, Phys. Lett. B **525**, 143 (2002); M. Fujii and K. Hamaguchi, Phys. Rev. D **66**, 083501 (2002); R. Jeannerot, X. Zhang and R. H. Brandenberger, JHEP **9912**, 003 (1999); W. B. Lin, D. H. Huang, X. Zhang and R. H. Brandenberger, Phys. Rev. Lett. **86**, 954 (2001).

[23] G. Belanger, F. Boudjema, A. Pukhov and A. Semenov, Comput. Phys. Commun. **149**, 103 (2002).

[24] M. Drees, M. M. Nojiri, D. P. Roy and Y. Yamada, Phys. Rev. D **56**, 276 (1997).

[25] M. Guchait and D. P. Roy, Phys. Rev. D **52**, 133 (1995).

[26] J. Ahrens *et al.* [The IceCube Collaboration], arXiv:astro-ph/0209556. http://icecube.wisc.edu/

[27] E. Aslanides *et al.* [ANTARES Collaboration], arXiv:astro-ph/9907432.

[28] P. Gondolo, J. Edsjo, P. Ullio, L. Bergstrom, M. Schelke and E. A. Baltz, arXiv:astro-ph/0211238.

[29] A. Bottino, F. Donato, N. Fornengo and S. Scopel, arXiv:hep-ph/0105233; *See also:* G. Duda, G. Gelmini, P. Gondolo, J. Edsjo and J. Silk, Phys. Rev. D **67**, 023505 (2003); G. Duda, G. Gelmini and P. Gondolo, Phys. Lett. B **529**, 187 (2002).

[30] J. R. Ellis, A. Ferstl and K. A. Olive, arXiv:hep-ph/0106148.

[31] R. Abusaidi *et al.* [CDMS Collaboration], Phys. Rev. Lett. **84**, 5699 (2000).

[32] H. V. Klapdor-Kleingrothaus, Nucl. Phys. Proc. Suppl. **110**, 58 (2002) [arXiv:hep-ph/0206250].

[33] R. Bernabei *et al.* [DAMA Collaboration], Phys. Lett. B **480**, 23 (2000).

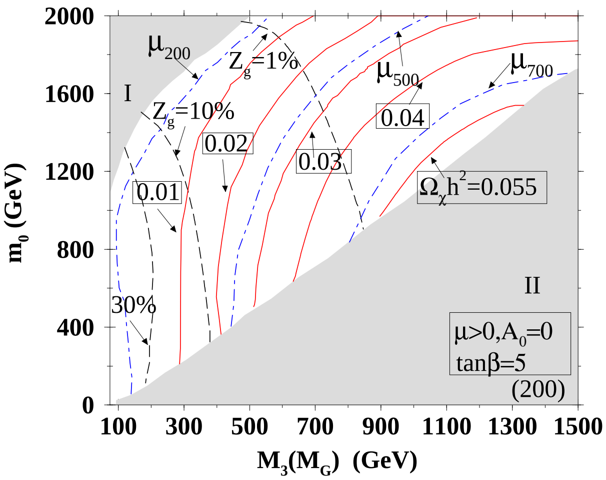

(a)

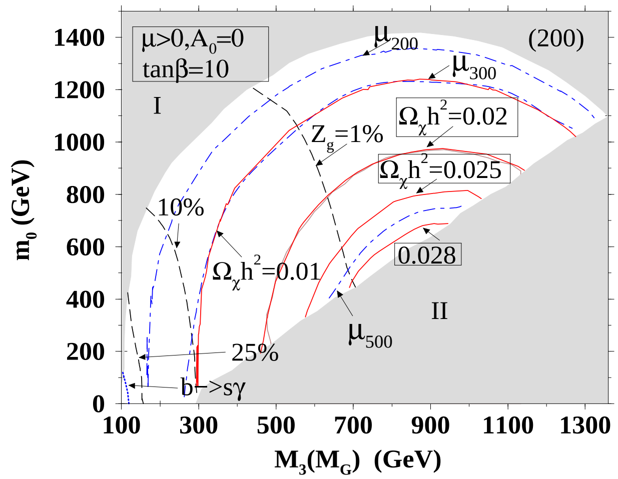

(b)

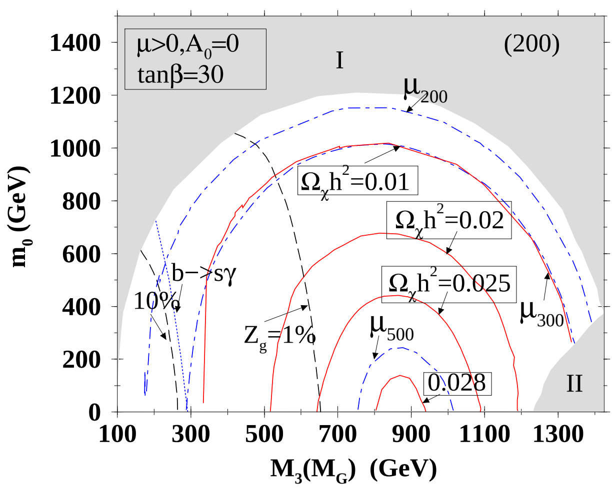

(c)

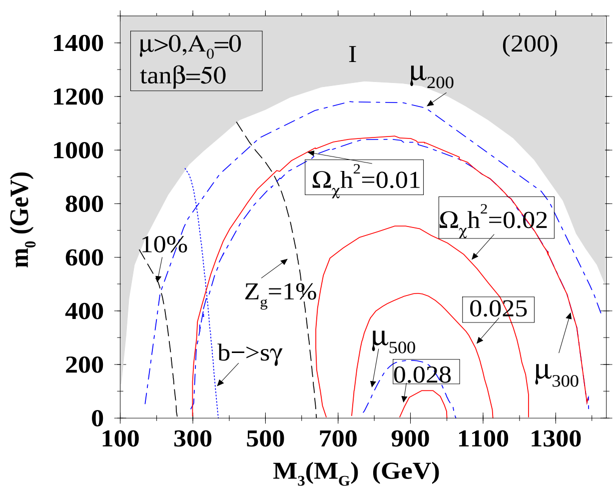

(d)

Figure 1: Contours of $\Omega_{\tilde{\chi}}h^2$, μ, Z_g and $Br(b \to s + \gamma)$ in the $(m_0 - M_3(M_G))$ plane for $\tan\beta = 5, 10, 30$ and 50 for the $n = 200$ nonuniversal gaugino mass model with $\mu > 0$. The neutralino relic density $\Omega_{\tilde{\chi}}h^2$ contours are shown as (red) solid lines. The contours for μ are shown as (blue) dot-dashed lines where the notation μ_{500} means $\mu = 500$ GeV. The gaugino fraction for the LSP Z_g contours are shown as (black) dashed lines. The $Br(b \to s + \gamma)$ excluded regions for each figure are the regions left to the (blue) dotted lines. The (gray) I-zones in the top left parts are discarded via the lighter chargino mass lower bound and the absence of radiative EWSB and (gray) II-zones are eliminated because of the lack of stability of the Higgs potential at the GUT scale M_G.

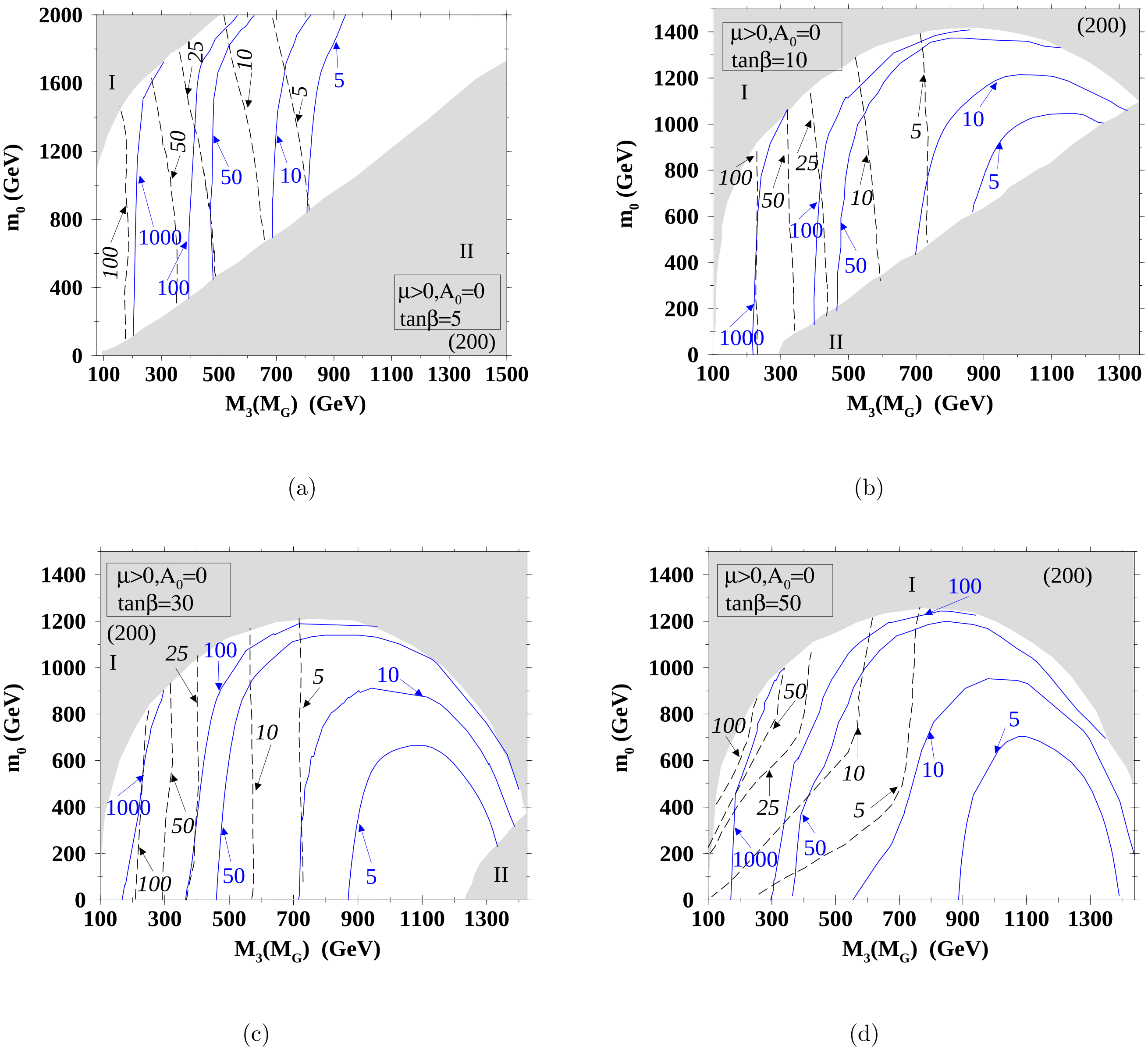

Figure 2: Contours for muon flux from the Sun in units of km^{-2}yr^{-1} for $\tan\beta = 5$, 10, 30 and 50 in the nonuniversal gaugino mass model with $n = 200$. The (blue) solid lines refer to ϕ_μ and the (black) dashed lines correspond to $\xi\phi_\mu$ where $\xi = \Omega_{\tilde{\chi}}h^2 / < \Omega_{\tilde{\chi}}h^2 >_{min}$, with $< \Omega_{\tilde{\chi}}h^2 >_{min} = 0.05$. The regions marked with I and II are same as that in Fig.1

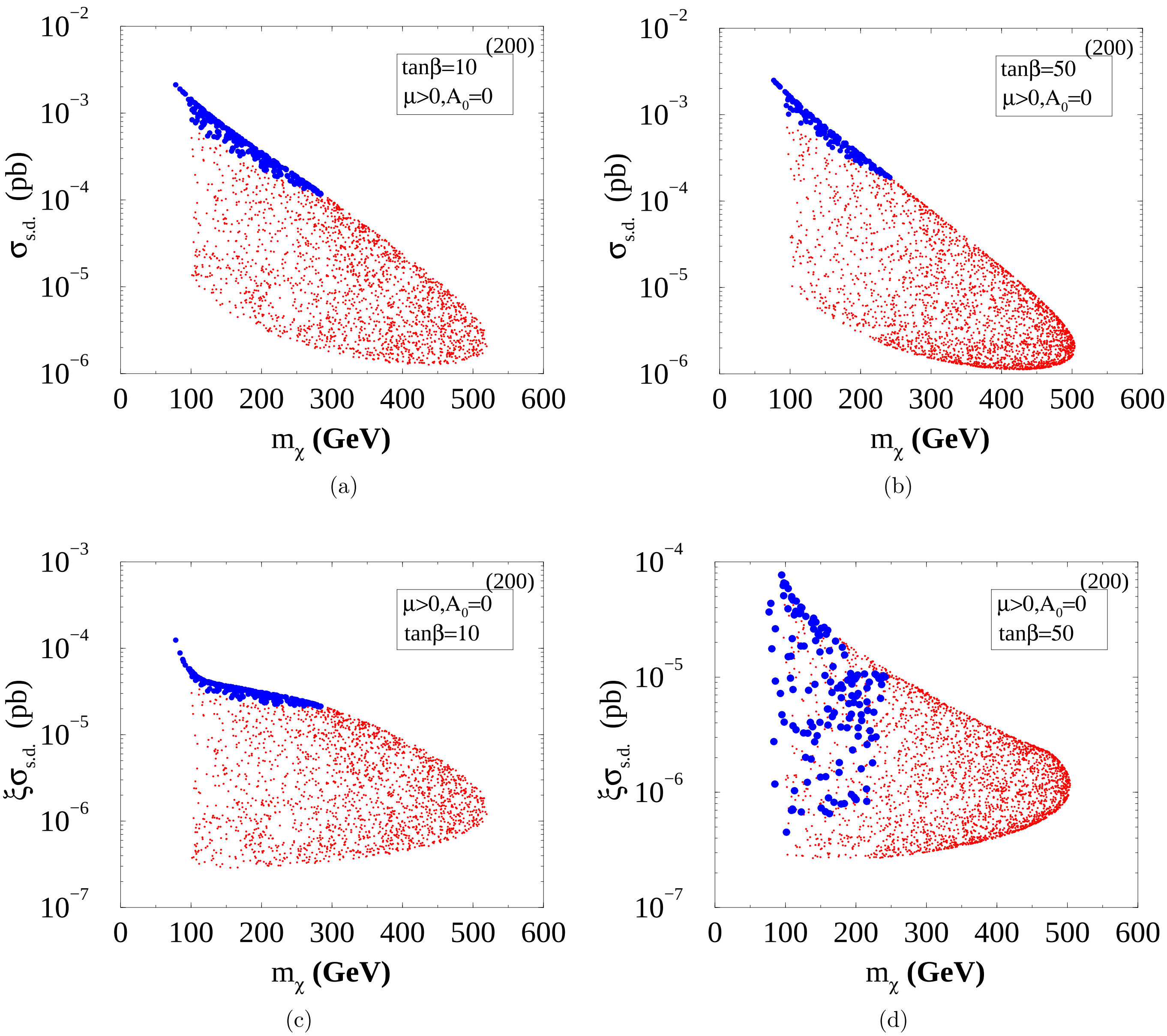

Figure 3: (a) and (b): Spin dependent neutralino-proton scattering cross sections $\sigma^{SD}_{\tilde{\chi}^0_1-p}$ vs $m_{\chi_1{}^0}$ for $\tan\beta = 10$ and 50 respectively for the $n = 200$ nonuniversal gaugino mass model. The (red) dots and the (blue) filled circles refer to points with below and above 10% gaugino fractions respectively in this generic Higgsino dominated LSP scenario. (c) and (d): Same as (a) and (b) except for the scaled cross sections $\xi\sigma^{SD}_{\tilde{\chi}^0_1-p}$, where $\xi = \Omega_{\tilde{\chi}}h^2/<\Omega_{\tilde{\chi}}h^2>_{min}$, with $<\Omega_{\tilde{\chi}}h^2>_{min} = 0.05$.

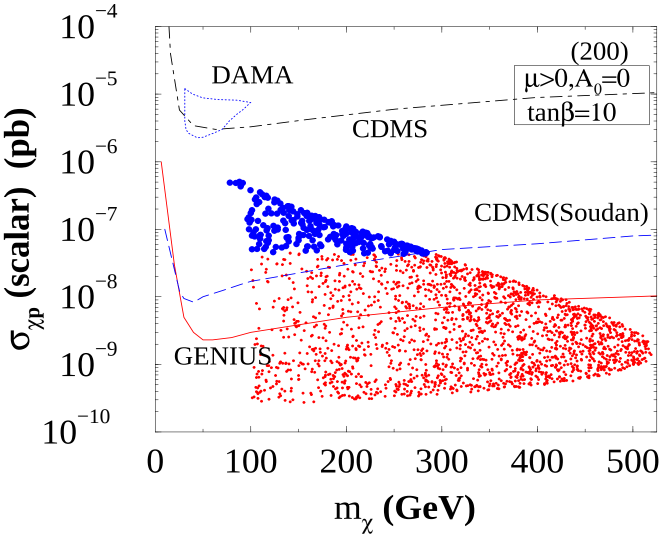

(a)

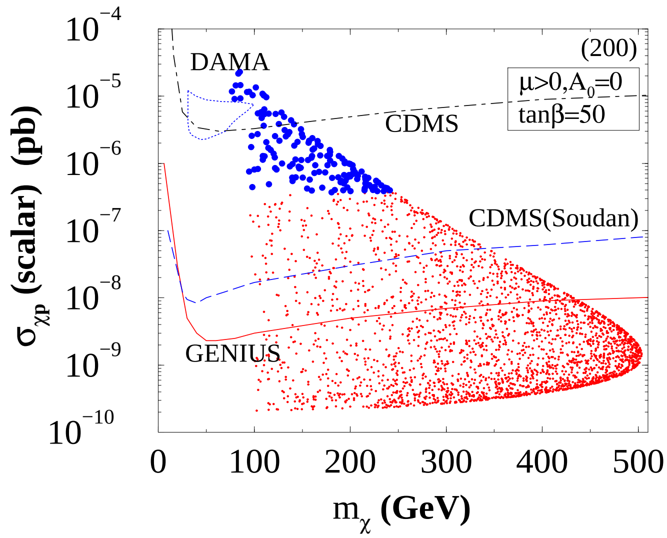

(b)

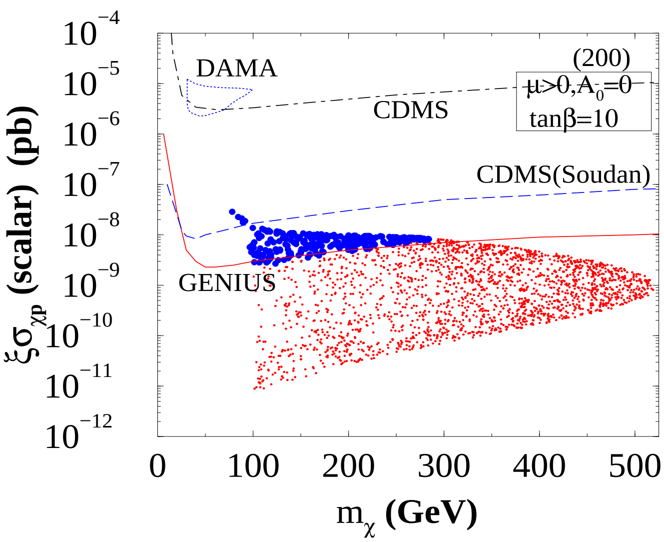

(c)

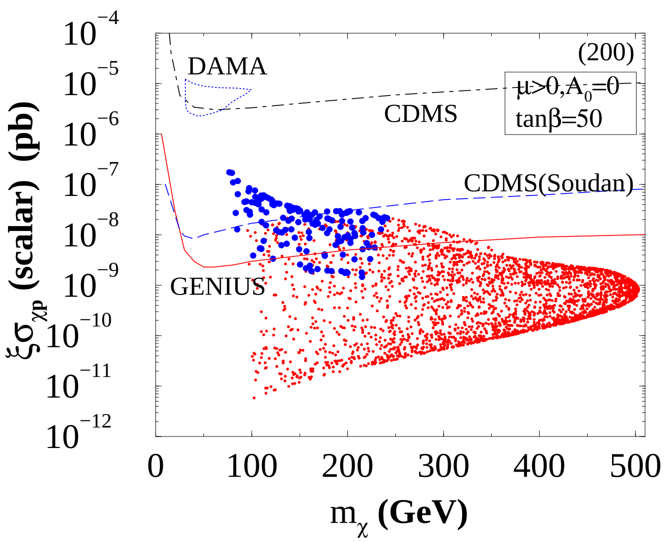

(d)

Figure 4: (a) and (b): Spin independent neutralino-proton scattering cross sections $\sigma_{\tilde{\chi}_1^0-p}$ vs $m_{\chi_1{}^0}$ for $\tan\beta = 10$ and 50 respectively for the $n = 200$ nonuniversal gaugino mass model. The (red) dots and the (blue) filled circles refer to points with below and above 10% gaugino fractions respectively in this generic Higgsino dominated LSP scenario. (c) and (d): Same as (a) and (b) except for the scaled spin independent cross sections $\xi\sigma_{\tilde{\chi}_1^0-p}$ where $\xi = \Omega_{\tilde{\chi}}h^2 / < \Omega_{\tilde{\chi}}h^2 >_{min}$, with $< \Omega_{\tilde{\chi}}h^2 >_{min} = 0.05$.